# SORPTION-ENHANCED REACTION PROCESS FOR ELECTRICITY PRODUCTION AND $CO_2$ CAPTURE

*Hendricus Th.J. Reijers, Gerard D. Elzinga, Steven C.A. Kluiters, Jan-Wilco Dijkstra, Paul D. Cobden and Ruud W. van den Brink,* Clean Fossil Fuels, Energy reseach Centre of the Netherlands, Westerduinweg 3, 1755 LE, Petten, Netherlands

*Introduction*

There is a growing awareness that energy must be produced at lower greenhouse gas emissions. Fossil fuels, though, will remain the most important energy source for the first half of this century. This has led to new technologies to reduce the emission of the $CO_2$ produced from the burning of fossil fuels. This $CO_2$ can be captured with end-of-pipe technologies from the flue gas of the energy production unit using a $CO_2$ scrubber, e.g. an amine solution. Other possibilities include the application of nitrogen-free combustion of fossil fuels which facilitate $CO_2$ capture, but require a costly nitrogen-oxygen separation step (Miracca et al. 2005). A third possibility is to use pre-combustion decarbonization. Here, the $CO_2$ produced is captured prior to combustion, while transferring the energy content of the fuel to hydrogen. Various pre-combustion routes for electricity production have been investigated, using a membrane reactor (Bracht et al. 1997, Pex et al. 2004) or the sorption-enhanced reaction process (= SERP) (Hufton et al. 1999, 2004). The relevant reaction(s) are:

$$CH_4 + H_2O \leftrightarrow CO + 3H_2 \quad (1)$$

$$CO + H_2O \leftrightarrow CO_2 + H_2 \quad (2)$$

for steam reforming of methane (SRM) only, and in addition

$$CH_4 + \tfrac{1}{2}O_2 \leftrightarrow CO + 2H_2 \quad (3)$$

$$CH_4 + \tfrac{3}{2}O_2 \leftrightarrow CO + 2H_2O \quad (4)$$

$$CH_4 + 2O_2 \leftrightarrow CO_2 + 2H_2O \quad (5)$$

for autothermal reforming of methane (ATRM). When the steam reforming or shift catalyst is mixed with a sorbent, as in the sorption-enhanced reaction process, the $CO_2$ produced in the above reactions is simultaneously adsorbed, so that the hydrogen production rate is enhanced. Thus, to obtain the same $CH_4$ conversion, the steam reforming process may be performed at lower temperatures compared with conventional reforming, typically between 450 and 550 ºC. Sorption-enhanced reforming is a batch process necessitating the regeneration of the sorbent which is saturated with $CO_2$. The preferred regeneration or purge gas is steam if the captured $CO_2$ is to be sequestrated. Compared with other purge gases (air, nitrogen or methane), steam can be easily separated from the purge stream. For continuous $H_2$ production using the reforming and/or water-gas shift reactions, more reactors must be available. An example of a sorption-enhanced reforming system for electricity production is shown in Figure 1. Both SERP reactors are filled with a mixture of steam reforming catalyst and $CO_2$ sorbent. A $CH_4/H_2O$ mixture is fed to reactor 1, purge gas to reactor 2 for regeneration. To improve the desorption

of $CO_2$, the temperature may be increased or the pressure may be decreased with respect to the temperature and pressure during adsorption. After the sorbent of reactor 1 is saturated with $CO_2$, the gas flows to both reactors are interchanged and $CO_2$ is desorbed from the bed of reactor 1, whereas steam reforming is performed in reactor 2. Part of the produced $H_2$ is fed to a gas turbine. The other part is used as fuel for the burner, which in turn drives the endothermic steam reforming reaction and the regeneration process.

The purpose of this paper is:

- to investigate its adsorption and desorption properties in more detail,
- to show the validity of the SERP concept for steam-reforming of methane,
- to select promising system configurations for SERP.

As to (1), emphasis is put on the relation between the purge gas to adsorbed $CO_2$ ratio on the one hand, and the sorbent properties and operation conditions on the other hand. As will be shown, the amount of purge steam for removal of $CO_2$ adsorbed by the bed is large and must be reduced to obtain an acceptable system efficiency.

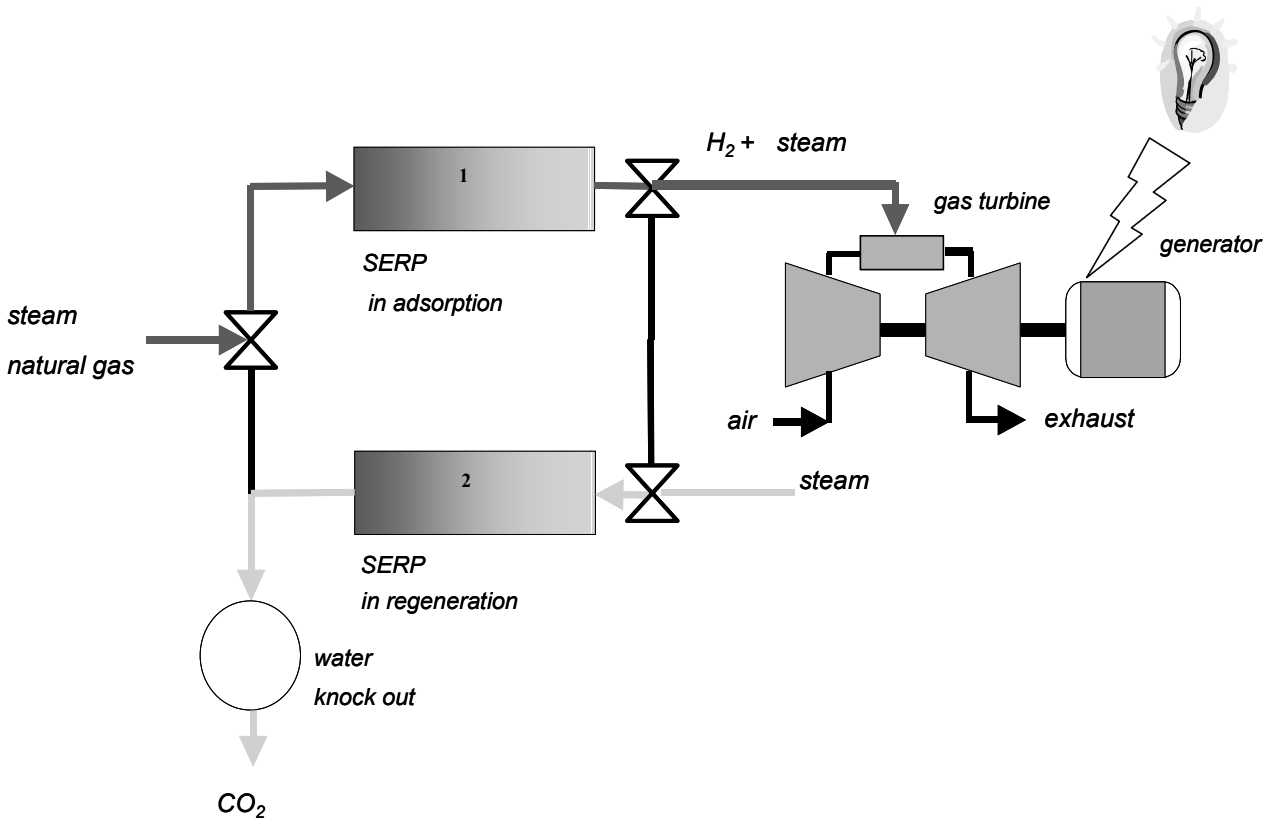


Figure 1 *Schematic representation of a SERP system for electricity production*

The purge steam/adsorbed $CO_2$ ratio needed to desorb a certain amount of $CO_2$, hereafter $S/CO_2$, will be experimentally determined. The plot of the desorbed fraction of $CO_2$ versus $S/CO_2$, is called the desorption characteristic. The steeper the characteristic, the more easily the $CO_2$ is desorbed. The relation between the purge steam/adsorbed $CO_2$ ratio for complete desorption, hereafter $(S/CO_2)_c$ and the properties of the chosen sorbent, promoted hydrotalcite, and operation conditions for sorption-enhanced steam reforming of methane is investigated in this paper.

*Hydrotalcites*

HTCs (= Hydrotalcites), also called layered double hydroxides or Feitknecht compounds, belong to the family of anionic clays. Their general formula is

$$M_{1-x}^{2+}M_{x}^{3+}(OH)_2(A^{n-})_{x/n}.mH_2O,$$

where $M^{2+}$ and $M^{3+}$ are divalent and trivalent metal ions respectively, and $A^{n-}$ is an anion. The value of x should be in the range 0.20 - 0.33. The metal ions and anions appear in different layers (Figure 2). The metal ion host layer has the brucite structure of $Mg(OH)_2$, in which the metal ions are octahedrally coordinated by $OH^-$ ions. Part of the divalent metal ions is replaced by trivalent ions, leaving the brucite structure intact. Consequently, this layer has a net positive charge which is compensated by the charge of the anion layer. The empty sites of the anion layer are filled with water molecules. The most common HTC is

$$(Mg)_{1-x}(Al)_x(OH)_2(CO_3)_{x/2}.mH_2O,$$

occurring in nature as $Mg_{0.75}Al_{0.25}(OH)_2(CO_3)_{0.125}.0.5H_2O$ (the mineral 'hydrotalcite') with which the above class of anionic clays is isostructural.

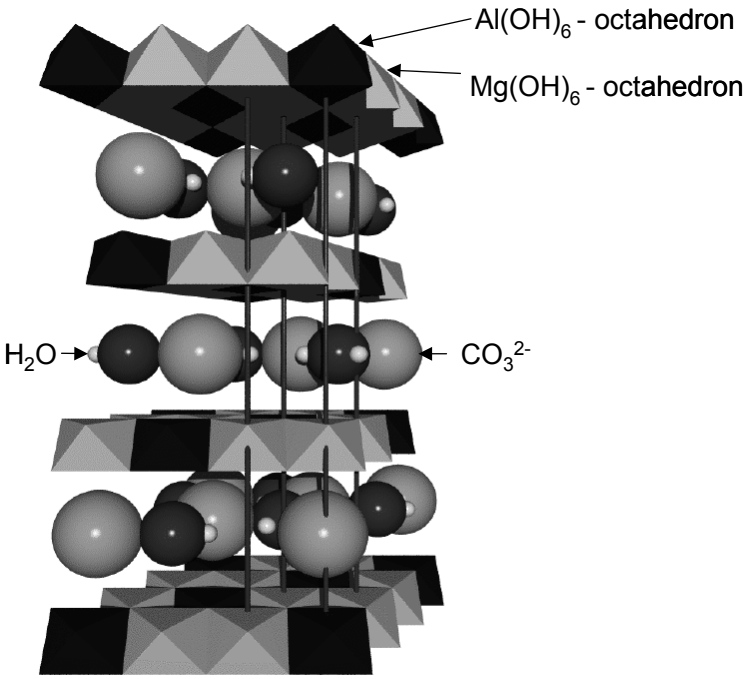


Figure 2 *Structure of hydrotalcite*

HTCs can be easily synthesized by coprecipitation from a solution of soluble salts containing the metal ions, usually at slightly elevated temperature and constant pH (Cavani et al. 1991). By slow addition of a carbonate salt, a precipitate is formed. The precipitate is separated by filtration and dried. Thanks to the structure of HTC, the metals are well mixed and dispersed and thus, HTCs are ideal candidate catalyst precursors. When the HTC is calcined in air or $N_2$, first it loses its interlayer water up to approximately 200 ºC. In the range 200 – 500 ºC, dehydroxylation and decarbonisation take place and the specific surface area

increases strongly. The suitability of calcined HTC as high temperature $CO_2$ sorbent stems from the plurality of strong basic sites at the surface this structure offers, which favours the adsorption of the acidic $CO_2$ according to the Lewis acid-base theory (Di Cosimo et al. 1998). When no further heating occurs, the thus obtained mixture of metal oxides can be transformed back into the original layered structure by contacting it with a salt solution. The anion (e.g. carbonate) is used for the interlayer between the metal ion host layers. This phenomenon is the so-called memory-effect of HTCs. HTCs used as $CO_2$ sorbent are usually promoted with alkali carbonates, which enhance the $CO_2$ adsorption considerably although the exact mechanism is still unknown.

*Experimental*

For our work, four commercially available HTCs (PURAL MG70, PURAL MG61 HT, PURAL MG50 and PURAL MG30) were obtained from SASOL. They are aluminum magnesium hydroxide carbonates of general formula $(Mg)_{1-x}(Al)_x(OH)_2(CO_3)_{x/2}.mH_2O$. Their specifications are given in Table 1. We also prepared several HTC samples in-house, called ECN-HTC. To a well-stirred $NaHCO_3$ solution of 65 ºC, a solution containing the metal nitrates in the ratio Mg/Al = 3 was added dropwise resulting in precipitation of the HTC precursor. The pH was kept at a constant value of 8.00 by adding a NaOH solution when needed. After that, the solution was allowed to cool down to room temperature overnight under vigorous stirring. Next day, the precipitate was separated from the suspension by filtration and dried for 24 hours at 120 ºC.

The HTC samples, both commercial and in-house prepared, were activated by heating them in air to 400 ºC and by keeping them at this temperature for 4 hours. After that, the obtained powders were loaded with 22 wt% $K_2CO_3$ using dry impregnation and dried overnight (Nataraj et al. 2000). The impregnated powders were compacted at a pressure of 275 atm and at room temperature. A sieve fraction of these particles was obtained with sizes between 0.212 and 0.425 mm. The experiments were performed using a glass reactor tube of 16 mm inner diameter and 150 mm length. The reactor was filled with 3 g of particles. The sample was heated under $N_2$ to the temperature of the experiment, usually 400 ºC. Humidified $N_2$ (29% $H_2O$) was passed along the sample for 75 minutes to remove any calcination products, the so-called pre-desorption step. After that, a series of adsorption/desorption cycles was applied. The conditions of the adsorption and desorption steps of a standard experiment are given in Table 2. The duration of both steps is 75 minutes and 60 gas samples per step from the dry effluent are analysed by a MicroGC (Hewlett Packard M200H), using a sample interval of 75 s. A permapure is used for drying the effluent. At the end of the experiment, the sample is cooled down to room temperature under dry $N_2$. The water is evaporated and mixed with the feed gas flow in a CEM (Controlled Evaporation Mixer) unit. The mass flow controllers, CEM unit and valves are computer-controlled. A schematic diagram is shown in Figure 3.

Table 1 *Specifications of HTCs according to the supplier*

| | spec. surface ($m^2/g$) | pore volume ($g/cm^3$) | bulk density ($g/cm^3$) | $MgO:Al_2O_3$ (wt%:wt%) |
|---|---|---|---|---|
| PURAL MG70 | > 180[1)] | > 0.2[1)] | 0.35 - 0.55 | 70:30 |
| PURAL MG61 HT | 16 | not specified | 0.15 | 61:39 |
| PURAL MG50 | > 200[1)] | > 0.2[1)] | 0.45 - 0.65 | 50:50 |
| PURAL MG30[2)] | > 250[1)] | > 0.5[1)] | 0.35 - 0.55 | 30:70 |

[1)] After 3 hours of activation at 550 ºC

[2)] PURAL MG30 contains a significant amount of boehmite

To determine the amount of $CO_2$ adsorbed and desorbed by the HTC samples only during respectively the adsorption and desorption steps, a so-called blank experiment was performed to correct for instrumental effects. For the blank experiment, a non-adsorbing material (SiC) of the same particle size range and bed volume as the adsorbing samples was used. The experimental conditions were identical to those applied in the adsorption and desorption steps of the experiments using an adsorbing sample. The following parameters were varied: HTC composition, $K_2CO_3$ loading, $H_2O$ fraction of the feed gas, promoter, operation temperature, desorption flow and desorption time. Finally, the HTC sorbent was mixed with a low-temperature steam reforming catalyst and a $CH_4/H_2O/N_2$ gas mixture was fed to the reactor to investigate sorption-enhanced reforming of methane.

Table 2 *Standard experimental conditions*

| | adsorption | desorption |
|---|---|---|
| flow (ml/min) | 30 | 100 |
| composition | 5% $CO_2$/29% $H_2O$/66% $N_2$ | 29% $H_2O$/71% $N_2$ |
| T (ºC) | 400 | 400 |
| duration (min) | 75 | 75 |

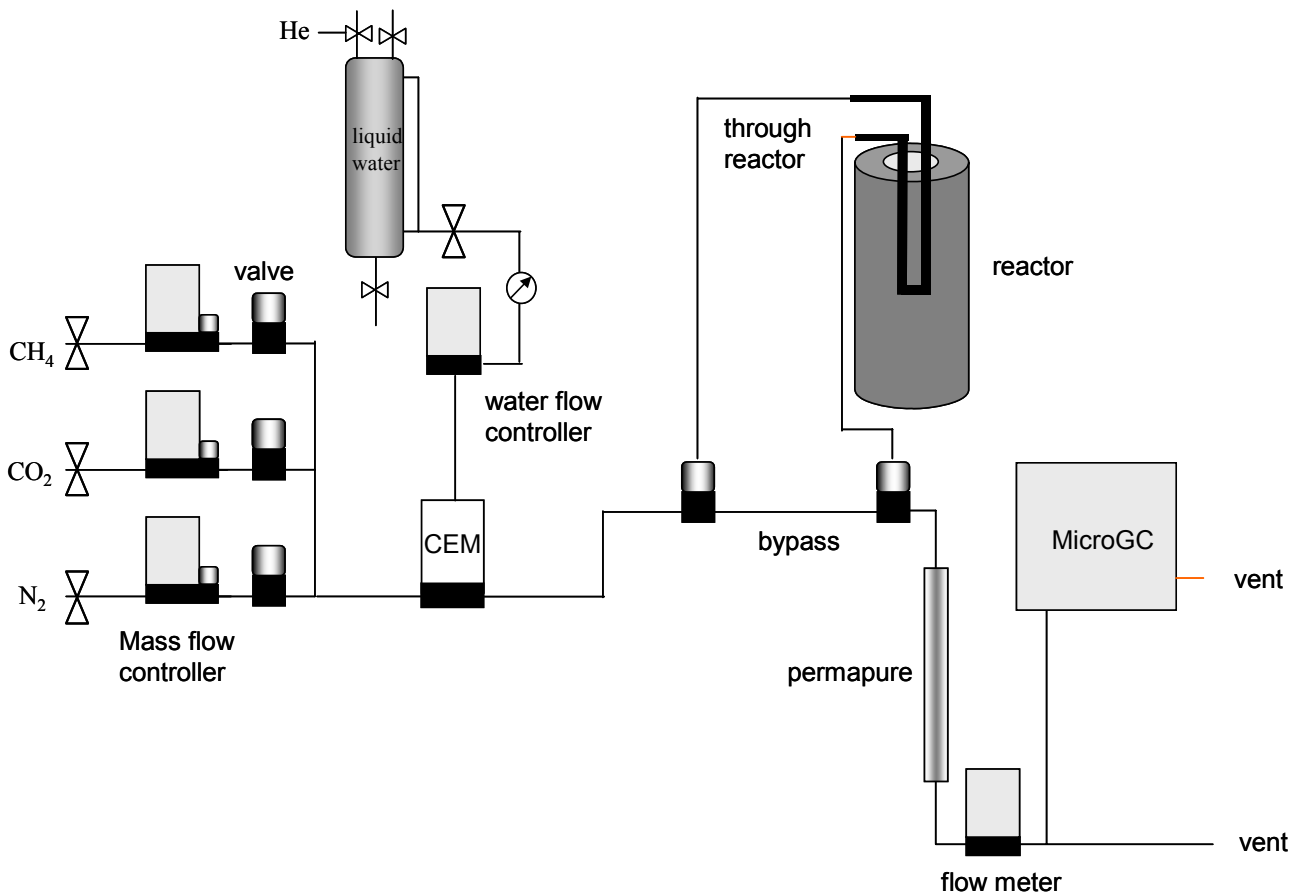


Figure 3 *Schematic diagram of the lab-scale experimental apparatus*

*Results and discussion*

Figure 4 shows the adsorption and desorption profiles corresponding with the 20th cycle of the experiments up to t = 40 min using the various PURAL samples and ECN-HTC, all loaded with 22 wt% $K_2CO_3$. The $CO_2$ adsorption decreases during the first 20 cycles for all samples. After the 20th cycle, it becomes approximately constant. The results of the blank experiments are indicated by dashed lines.

Table 3 *$CO_2$ adsorption capacities at breakthrough and during the whole adsorption step at various conditions for the 20th cycle*

| | $t_{bt}$ (min) | $q_{ads}(t_{bt})$ (mmol/g) | $q_{ads}$(t=75 min) (mmol/g) |
|---|---|---|---|
| HTC sample | | | |
| PURAL MG70 | 7.5 | 0.14 | 0.33 |
| PURAL MG61 HT | 8.8 | 0.18 | 0.28 |
| PURAL MG50 | 7.9 | 0.17 | 0.33 |
| PURAL MG30 | 12.5 | 0.29 | 0.44 |
| Mg-Al HTC | 9.0 | 0.18 | 0.35 |
| $K_2CO_3$ loading (wt%) | | | |
| 0 | 2.5 | 0.02 | 0.06 |
| 11 | 6.4 | 0.13 | 0.18 |
| 22 | 6.9 | 0.14 | 0.18 |
| 33 | 6.4 | 0.12 | 0.16 |
| 44 | 5.2 | 0.09 | 0.13 |
| $H_2O$ content of feed gas (%) | | | |
| 0 | 5.0 | 0.10 | 0.21 |
| 7.5 | 6.1 | 0.13 | 0.29 |
| 15 | 8.8 | 0.20 | 0.33 |
| 29 | 8.8 | 0.21 | 0.33 |
| temperature (ºC) | | | |
| 400 | 8.8 | 0.18 | 0.33 |
| 450 | 8.7 | 0.18 | 0.32 |
| 500 | 7.5 | 0.14 | 0.27 |

The adsorption profiles of PURAL MG70, MG61 HT and ECN-HTC are similar (breakthrough times respectively 7.5 min, 8.8 min, 9.0 min), whereas that of PURAL MG50 starts to break through at the same time as the before-mentioned ones (7.9 min) though it rises less strongly, whereas breakthrough of PURAL MG30 clearly occurs at a later time (12.5 min). For all samples we find that after breakthrough, the profile does not show a sharp rise towards the inlet $CO_2$ flow (1.5 ml/min), but rather slowly creeps to this value. Table 3 shows the calculated amount of $CO_2$ adsorbed up to the breakthrough time $t_{bt}$ and during the whole adsorption step (here 75 min), respectively $q_{ads}(t_{bt})$ and $q_{ads}$(t=75min). About two thirds of all $CO_2$ is adsorbed before breakthrough. The desorption profiles show a rapid initial $CO_2$ release, which considerably slows down during deeper desorption and never becomes zero. At the end of the desorption step, the $CO_2$ flow is in the range 0.05 - 0.1 ml/min. Apart from the desorption peak, which is highest for PURAL MG30, the profiles of the various samples are quite similar. The desorbed amount exceeds the adsorbed amount of $CO_2$. During impregnation of calcined HTC with $K_2CO_3$, the original HTC structure is partly restored due to the memory effect (Cavani et al. 1991). When the impregnated HTC is heated again, calcination of the restored structure occurs which is apparently not complete after the pre-desorption step.

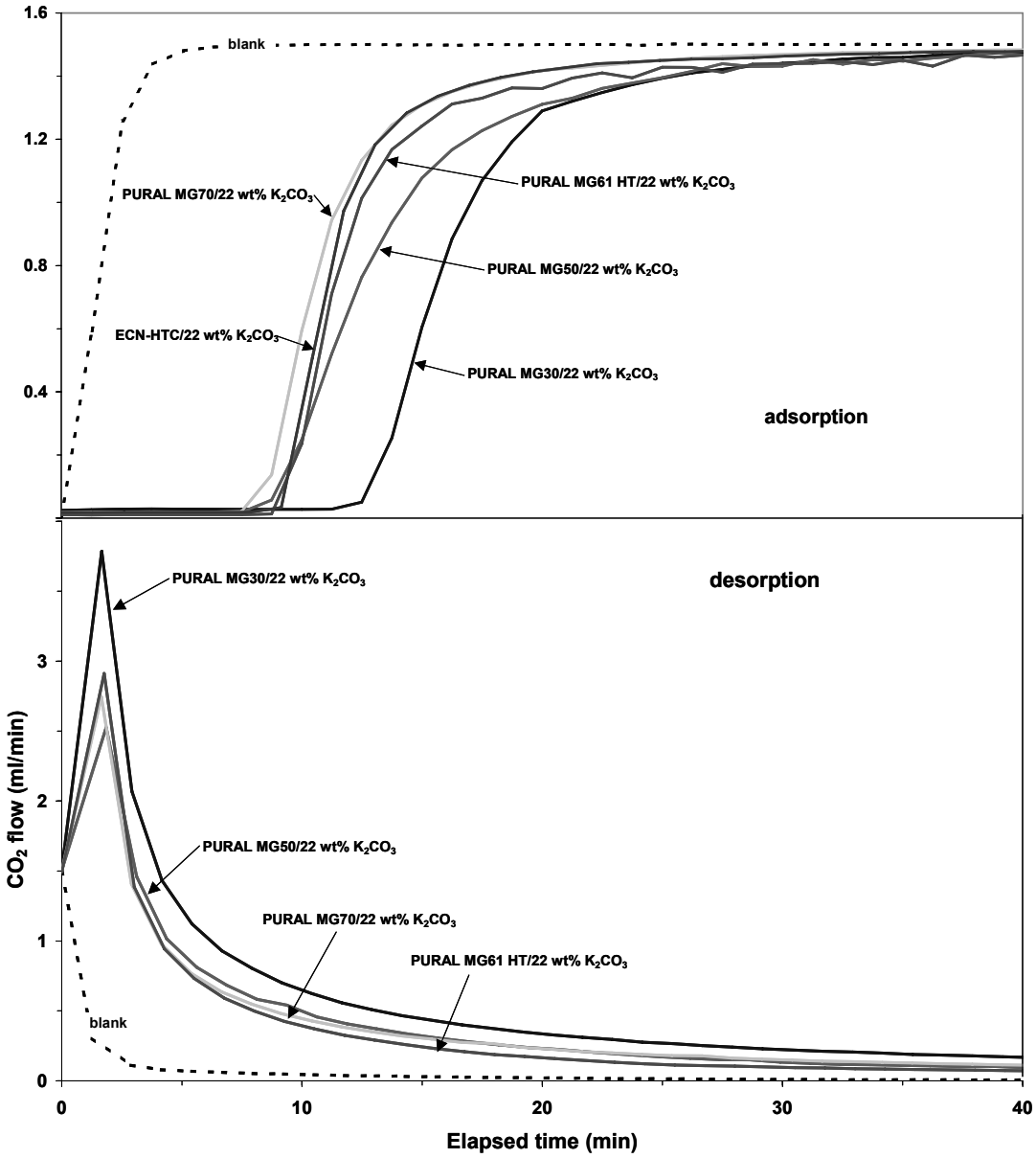


Figure 4 *Adsorption and desorption profiles of various potassium- promoted HTC samples (the desorption profiles of ECN-HTC/22 wt% $K_2CO_3$ coincides with that of PURAL MG70/22 wt% $K_2CO_3$)*

Figure 5 shows the adsorption and desorption profiles corresponding with the 20$^{th}$ cycle of experiments using PURAL MG70 with different $K_2CO_3$ loadings. For comparison, also the unloaded sample is included. It is seen that the $CO_2$ adsorption is enhanced by a factor 3 when loading the HTC with $K_2CO_3$, implying that the original HTC structure is not simply restored upon contacting the calcined product with $K_2CO_3$. The $CO_2$ adsorption is not very sensitive to the loading percentage (Table 3). The desorption profiles of the various samples are quite similar. The shift of the peak position is due to the extent of sorbent loading, not to differences in desorption properties of the various samples.

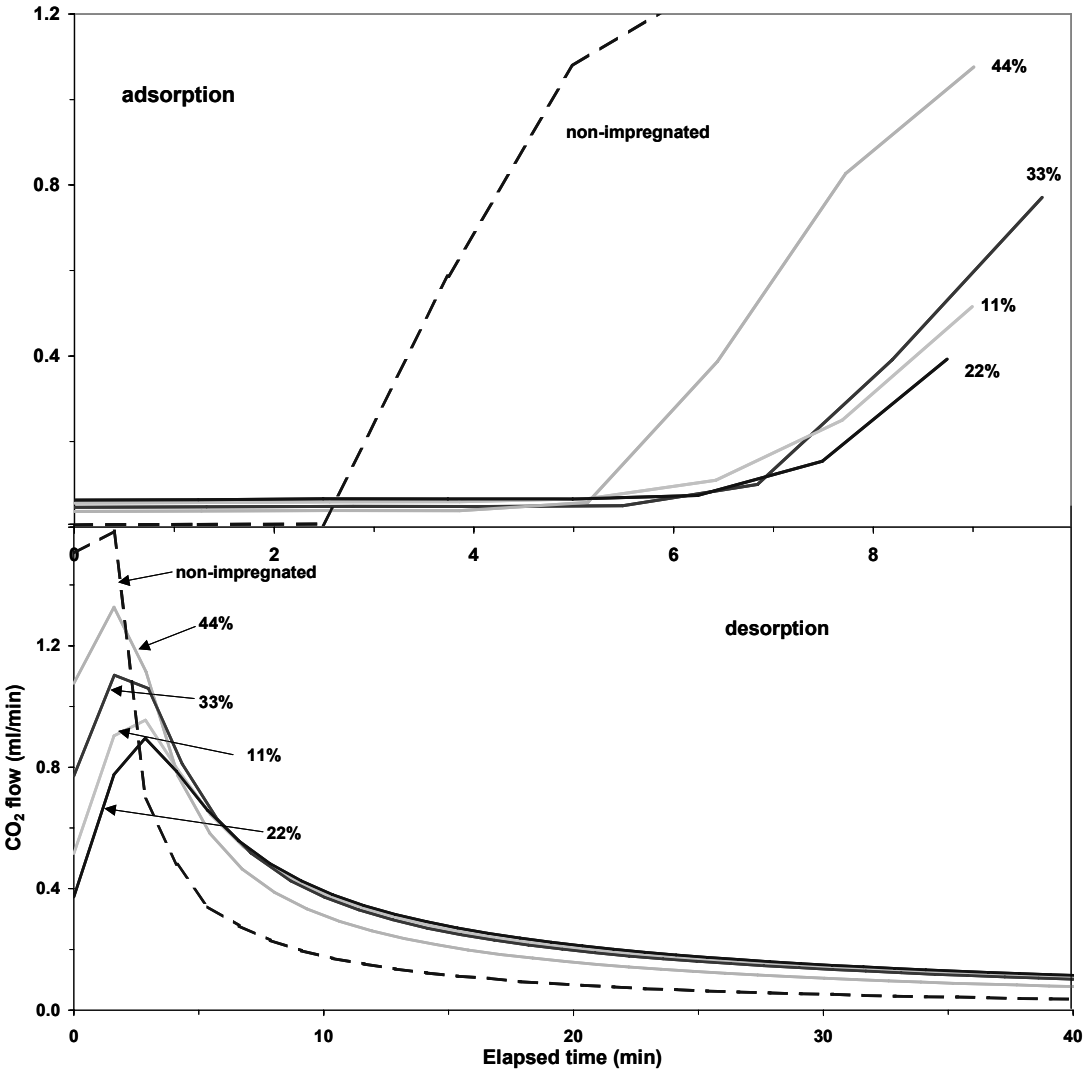


Figure 5 *Adsorption and desorption profiles of PURAL MG70 with different $K_2CO_3$ loadings*

The presence of water during adsorption is important. Without water, the $CO_2$ adsorption capacity is smaller than in the presence of water. At $H_2O$ fractions in the feed gas of 15% or higher, the $CO_2$ adsorption does not increase (Table 3). The temperature of the experiment, which refers to both the temperature of activation and the temperature at which the series of adsorption and desorption cycles is performed, does not have a strong effect on the $CO_2$ adsorption capacity. From 400 to 450 ºC, it hardly varies, while it has slightly decreased at 500 ºC (Table 3).

As pointed out in the introduction, $S/CO_2$, the purge gas to adsorbed $CO_2$ ratio, is an important parameter. The desorption characteristic yields the variation of the fraction of desorbed $CO_2$ with $S/CO_2$. The desorption flow and period have been decreased stepwise to reduce the value of $S/CO_2$ for complete desorption, $(S/CO_2)_c$. Figure 6 shows the desorption characteristics of PURAL MG70 loaded with 22 wt% $K_2CO_3$, determined at different desorption periods ($t_{ads}$ = 10 min, $t_{des}$ = 10, 25, 50, 75 min, $F_{ads} = F_{des}$ = 30 ml/min). Decreasing the desorption flow implies that the required amount of purge gas decreases more strongly than the amount of adsorbed $CO_2$, so that $(S/CO_2)_c$ shows a net decrease. When the desorption

flow is decreased from 100 to 10 ml/min, $(S/CO_2)_c$ drops by approximately a factor 5. The $(S/CO_2)_c$ decreases by a about factor 3 when $t_{des}$ is reduced from 75 to 10 minutes. This indicates that the smaller part of the bed which is used, the more easily the adsorbed $CO_2$ can be removed from the bed.

Finally, to deliver a proof-of-the-principle test for sorption-enhanced steam reforming of methane, an experiment has been performed using a mixture of 1.5 g low-temperature steam reforming catalyst and 3.0 g PURAL MG70 impregnated with 22 wt% $K_2CO_3$. As before, the sample was subjected to a series of reaction/regeneration cycles at 400 ºC. Feed gas containing 2.9 % $CH_4$, 17.4% $H_2O$ and balance $N_2$ at a flow rate of 25 ml/min was fed to the sample during the reaction step, while the standard feed gas was used for regeneration (Table 2). The results of the last ($100^{th}$) cycle are shown in Figure 7. More $H_2$ is produced during reaction than predicted by thermodynamic equilibrium without sorbent. An average $CH_4$ conversion of 95% is obtained (thermodynamic equilibrium conversion of $CH_4$ without sorbent: 53%), demonstrating the suitability of HTC for sorption-enhanced reforming of methane.

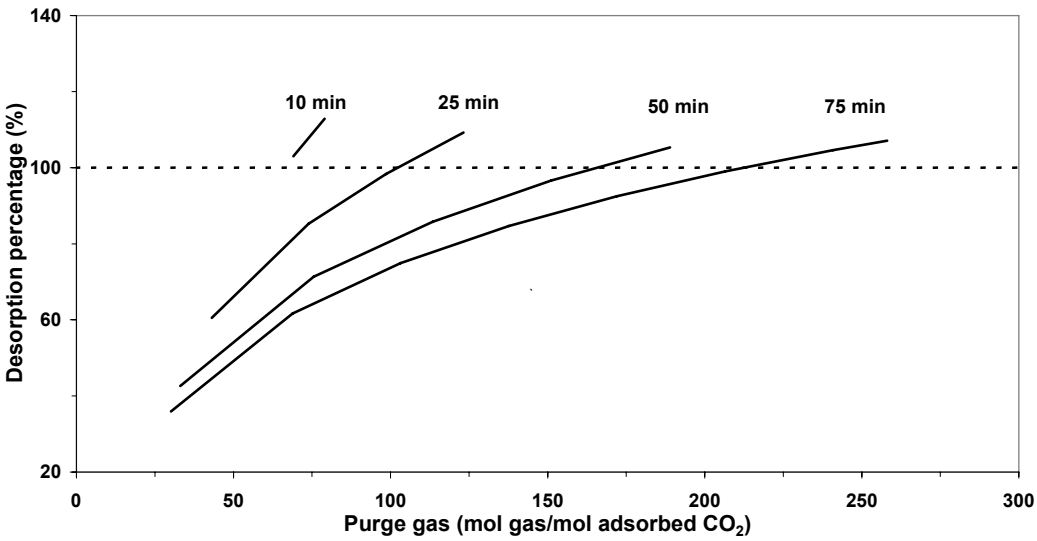


Figure 6 *Desorption characteristics determined for different desorption times indicated in the figure ($t_{ads}$ = 10 min, $F_{des}$ = 30 ml/min)*

*Systems studies*

Systems studies have been performed to compare the performance of a SERP-based electricity production system with that of a similar one using conventional, post-combustion amine scrubber for $CO_2$ capture. Table 4 shows the investigated systems:

- SE-WGS (sorption-enhanced water-gas shift), where SERP is restricted to the water-gas shift reactor only, which is preceded by an ATR (autothermal reforming) reactor and a conventional water gas shift reactor, and
- SE-SMR (sorption-enhanced steam-reforming of methane), where SERP is used in combination with an SMR (steam methane reforming) reactor.

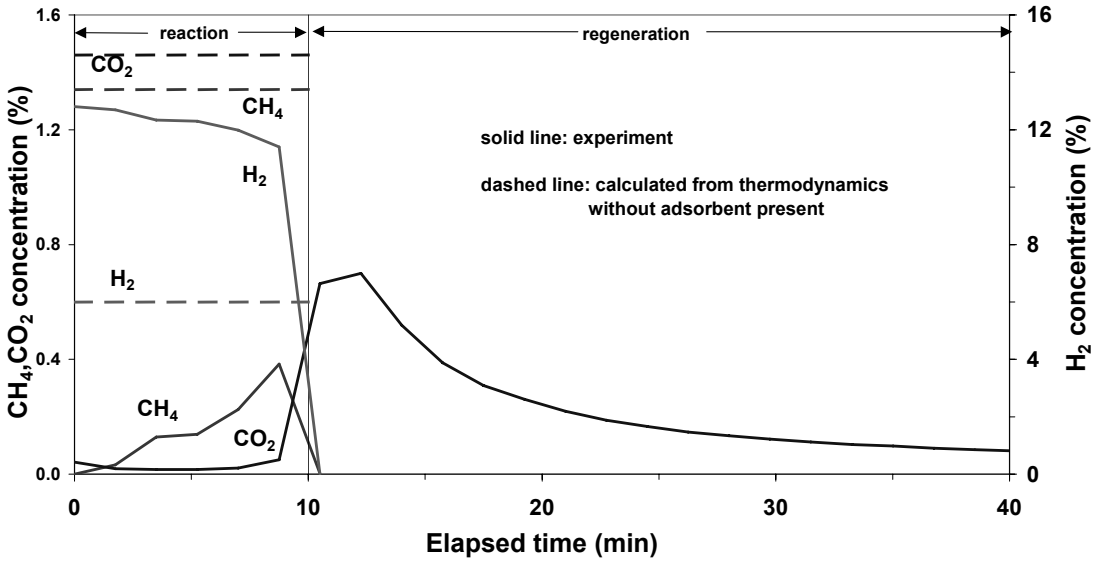


Figure 7 *Effluent gas composition during reaction and regeneration using a mixture of steam reforming catalyst and HTC impregnated with 22 wt% $K_2CO_3$*

For the first system, two options were investigated: air and $O_2$ blown ATR. In the latter system, a water-gas shift reactor is not required. Two sorbents have been used: HTC and CaO, which are regenerated by pressure swing and temperature swing respectively. Since the temperature ranges where $CO_2$ adsorption is effective, differ for these sorbents (400 - 500 ºC for HTC, and 600 - 700 ºC CaO), CaO is excluded from SE-WGS. The SE-SMR system is shown in Figure 8. For the air-blown SE-WGS system, a side branch configuration is used, where compressed air from the gas turbine is fed to the ATR reactor. As reference, a gas turbine combined cycle based on a Siemens V94.3A turbine of nominal power output 380 MWe and efficiency 57.1% is used. The efficiency penalty due to $CO_2$ capture (86.2% carbon capture ratio) using an amine scrubber, amounts to 9.1%.

Table 4 *Investigated sorbent/system combinations*

| sorbent | system | |
|---|---|---|
| | air/$O_2$ SE-WGS | SE-SMR |
| HTC | x | x |
| CaO | | x |

Assumptions with regard to adsorption and desorption conditions are summarized in Table 5. ‘$CH_4$ conv.’and ‘CO conv.’ are the conversion of $CH_4$ and CO respectively, ‘S/C’ is the steam-to-carbon ratio of the feed gas, ‘S/$CO_2$’ is the steam-to-adsorbed $CO_2$ ratio required for bed regeneration. The values of ΔH are taken from Ding and Alpay (HTC, Ding and Alpay 2000) and from a thermodynamic database (CaO, Roine 2002). The operation conditions of the SE-WGS systems are taken from Air Products (Allam et al. 2005), the $CH_4$ and CO conversions and S/C of CaO-based SE-SMR are taken from Meyer (Meyer at al. 2005). The adsorption pressure is determined by the operation pressure of the combustion chamber of the gas turbine. For the other parameters, reasonable values have been assumed.

The following general assumptions were made:

- Natural gas is used as fuel.
- There is no export steam or export $H_2$.
- A single-pressure level steam cycle is used.
- Constant isentropic efficiencies are used.
- The pressure does not vary over the system components except for compressors and turbines.
- The captured $CO_2$ is compressed to 110 bar.

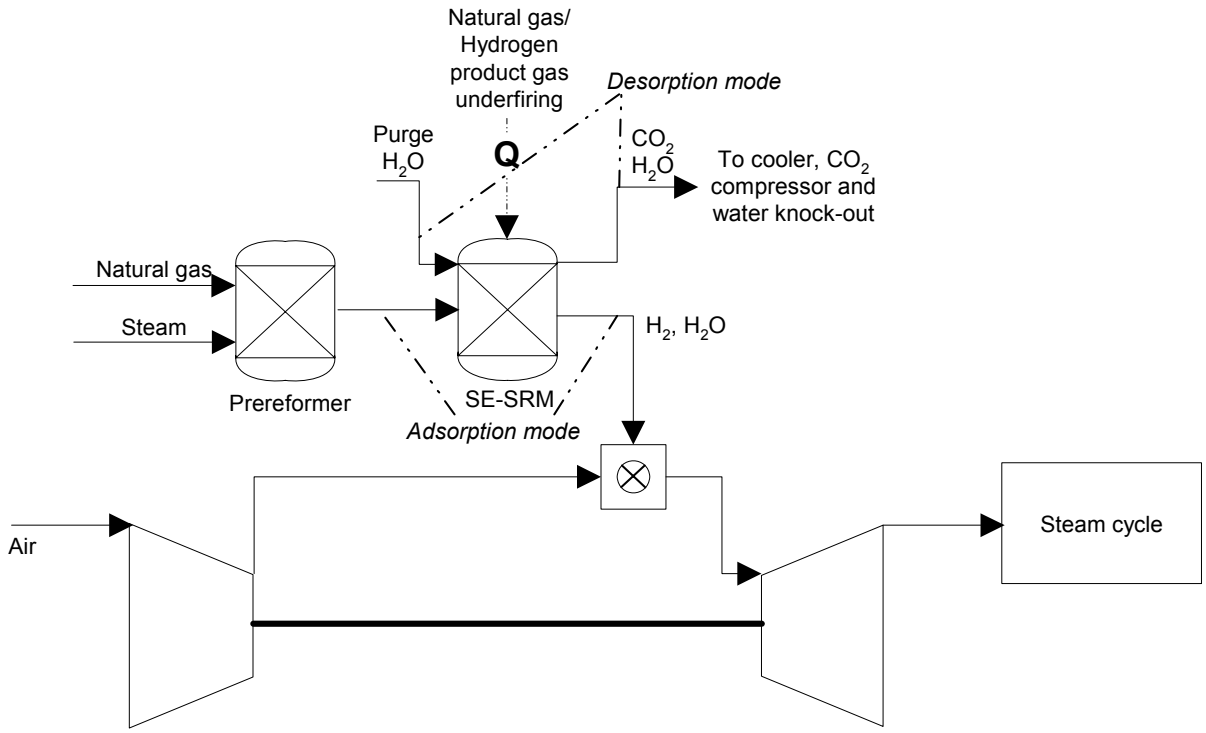


Figure 8 *SE-SMR system*

A summary of the results is shown in Table 6. The efficiency is defined as the net export electricity divided by the lower heating value fuel input. The CCR (carbon capture ratio) is the fraction of recovered $CO_2$. For SE-SMR system, part of the $H_2$ rich product gas from the SERP reactor has been used for underfiring, as a supplement of natural gas, to increase the CCR to 85%, though with associated efficiency penalty.

For all cases, the obtained efficiencies exceed that of the reference with $CO_2$ capture (48%). The highest efficiency is obtained for CaO-based SE-SMR, though the CCR is 5% points lower than that of the SE-WGS systems. The efficiency proves to be sensitive to the amount of steam needed for the process, thus it depends on the S/C and $S/CO_2$ values.

For the above calculations, the reformer or water-gas shift reactor is considered as a 'black box'. The actual layout can be quite complex as shown by e.g. the configuration developed by Air Products for the SE-WGS system (Allam et al. 2005). For the systems requiring a temperature swing for desorption (CaO-based systems), a fluidized-bed tandem configuration is anticipated (Meyer et al. 2005). The workability of this reactor concept is a point of further research. Experiments must show if the low $S/CO_2$ values allow long operation

times of the catalyst/adsorbent bed. Finally, a cost analysis of the investigated systems must be performed to allow a selection on the basis of lowest $CO_2$ removal cost per ton of avoided $CO_2$.

Table 5 *Operation conditions of investigated systems ('-' means not applicable)*

| | air/SE-WGS | $O_2$/SE-WGS | SE-SMR | SE-SMR |
|---|---|---|---|---|
| sorbent | HTC | HTC | HTC | CaO |
| **Adsorption** | | | | |
| $CH_4$ conv. (%) | - | - | 93 | 93 |
| CO conv. (%) | 95 | 95 | 96.8 | 96.8 |
| S/C (-) | 1.5 | 1.5 | 3.0 | 3.0 |
| T (ºC) | 400 | 400 | 400 | 600 |
| p (bar) | 17 | 17 | 17 | 17 |
| ΔH (kJ/mol) | 17 | 17 | 17 | 170 |
| **Desorption** | | | | |
| S/$CO_2$ (-) | 1.8 | 1.8 | 1.8 | 1.8 |
| T (ºC) | 400 | 400 | 400 | 1000 |
| p (bar) | 2.8 | 2.8 | 2.8 | 17 |
| ΔH (kJ/mol) | -17 | -17 | -17 | -170 |

Table 6 *Results of systems studies ('-' means not applicable)*

| | air/SE-WGS | $O_2$/SE-WGS | SE-SMR | SE-SMR | base case | base case |
|---|---|---|---|---|---|---|
| sorbent | HTC | HTC | HTC | CaO | - | amine |
| Efficiency (%) | 50.4 | 48.5 | 51.6 | 52.6 | 57.1 | 48.0 |
| CCR (%) | 90.0 | 90.0 | 85.0 | 85.0 | 0 | 86.2 |

*Conclusions*

The selected high temperature $CO_2$ sorbent, Mg-Al HTC, is able to adsorb $CO_2$ at temperatures between 400 and 500 ºC. The adsorption is considerably enhanced by impregnating this HTC with $K_2CO_3$. Loadings between 11 and 44 wt% have been tested, but the adsorption proved not to be very sensitive to the loading percentage. The adsorption, at least the part after breakthrough, and desorption profiles of the potassium-promoted HTC consist roughly of two parts: a part characterized by fast adsorption (desorption) and a part characterized by slow adsorption (desorption). In the performed experiments, desorption was never complete. The end of the desorption profiles did not go to zero and the desorbed amounts of $CO_2$ exceeded the adsorbed amounts of $CO_2$. This is most probably due to $CO_2$ released from the HTC structure. Water assists the $CO_2$ adsorption and desorption process. In the investigated temperature range, 400 - 500 ºC, the $CO_2$ loading capacity hardly varies. Lowering the desorption flow or the duration of the desorption step, results in smaller values of $(S/CO_2)_c$. An actual sorption-enhanced reforming experiment, in which the promoted htc was mixed with a catalyst, showed that methane conversions of 95% at 400 °C are reached. This is well above the equilibrium conversion at this temperature (55%).

All investigated systems show an efficiency gain with respect to the reference system (GTCC with amine scrubber). The highest efficiency is obtained for the CaO-based SE-SMR

system. The efficiency is very sensitive to the $S/CO_2$ value. Critical issues are the reactor concept and the low $S/CO_2$ value.

Summarizing, systems calculations show that sorption enhanced reforming is a technology with the possibility to capture $CO_2$ with low efficiency penalties. Lab-scale experiments have shown that high methane conversions can be reached at low temperatures, while simultaneously capturing $CO_2$.

*Acknowledgements*

This research has been carried out by ECN in the CATO-project (Carbon Capture, Transport and Storage), which is financed by the BSIK subsidy program of the Dutch Government agency SenterNovem. It is also part of ECN's DECAFF-program (Decarbonisation of Fossil Fuels), which is sponsored by the Dutch ministry of Economic Affairs.

*References*

Allam, R.J.; Chiang, R.; Hufton, J.R.; Middleton, P.; Weist, E.L.; White, V. Chapter 13 Development of the sorption enhanced water gas shift process. In *Carbon Dioxide Capture for Storage in Deep Geologic Formations - Results from the $CO_2$ Capture Project, Volume 1*. Thomas, D.C. and Benson, S.M. (Eds.); Elsevier: Oxford, 2005.

Bracht, M. Water gas shift membrane reactor for $CO_2$ control in IGCC systems: techno-economic feasibility study. *Energy Conv. Management*, **1997**, *38* (supplement), 159-162.

Cavani, F.; Trifirò, F.; Vaccari, A. Hydrotalcite-type anionic clays: preparation, properties and applications. *Cat. Today*, **1991**, *11*, 173-301.

Di Cosimo J.I.; Diez, V.K.; Xu, M.; Iglesia, E.; Apesteguia, C.R. Structure and surface and catalytic properties of Mg-Al based basic oxides. *J. Cat.* **1998**, *178*, 499-510.

Ding,Y.; Alpay, E. Equilibria and kinetics of high temperature CO2 adsorption on hydrotalcite adorbent, *Chem. Eng. Science*, **2000**, *55*, 3461-3474.

Miracca, I.; Aasen, K.J.; Brownscombe, T.; Gerdes, K.; Simmonds, M. Chapter 25 Oxyfuel Combustion for $CO_2$ Capture Technology Summary. In *Carbon Dioxide Capture for Storage in Deep Geologic Formations - Results from the $CO_2$ Capture Project, Volume 1*; Thomas, D.C and Benson S.M (Eds.); Elsevier: Oxford, 2005.

Hufton, J.R.; Mayorga, S.; Sircar, S. Sorption-enhanced reaction process for hydrogen production. *AIChE Journal*, **1999**, *45*, 248-256.

Hufton, J.R.; Allam, R.J.; Chiang, R.; Middleton, P.; Weist, E.L.; White, V. Development of a process for $CO_2$ capture from gas turbines using a sorption enhanced water gas shift reactor system, in *Proceedings of the 7th International Conference on Greenhouse Gas Technologies*, Vancouver, British Columbia, Canada, 5-9 September 2004, http://www.carbonsq.ca.

Meyer,J., R.J.Aaberg, and B.Andresen. Chapter 12 Generation of hydrogen fuels for the thermal power plant with integrated CO2 capture using a CaO-CaCO3 cycle. In *Carbon Dioxide Capture for Storage in Deep Geologic Formations - Results from the $CO_2$ Capture Project, Volume 1*. Thomas, D.C. and Benson, S.M. (Eds.); Elsevier: Oxford, 2005.

Nataraj, S.; Carvill, B.T.; Hufton, J.R.; Mayorga, S.G.; Gaffney, T.R.; Brzozowski, J.R. Materials selectively adsorbing $CO_2$ from $CO_2$ containing streams. Air Products and Chemicals Inc., EP Patent no. 1006079A1, **2000**.

Pex, P.P.A.C.; Delft, Y.C. van; Corrreia, L.A.; Veen, H.M. van; Jansen, D.; Dijkstra, J.W. Membranes for hydrogen production with $CO_2$ capture. In *Proceedings of the 7th International*

*Conference on Greenhouse Gas Technologies*, Vancouver, British Columbia, Canada, 5-9 September 2004, http://www.carbonsq.ca, or: http://www.ecn.nl/library/confe/conf2004.html.
Roine, A. HSC Chemistry, Outokumpu (version 5.0), 2002.